



C16orf72/HAPSTR1 is a molecular rheostat in an integrated network of stress response pathways

David R. Amici^{a,b}, Daniel J. Ansel^{a,b}, Kyle A. Metz^{a,b}, Roger S. Smith^{a,b}, Claire M. Phoumyvong^{a,b}, Sitaram Gayatri^{a,b}, Tomasz Chamera^c, Stacey L. Edwards^c, Brendan P. O'Hara^{a,b}, Shashank Srivastava^{a,b}, Sonia Brockway^{a,b}, Seesha R. Takagishi^{a,b}, Byoung-Kyu Cho^d, Young Ah Goo^d, Neil L. Kelleher^d, Issam Ben-Sahra^{a,b}, Daniel R. Foltz^{a,b}, Jian Li^e, and Marc L. Mendillo^{a,b,1}

Edited by Jonathan Weissman, Whitehead Institute, Cambridge, MA; received June 17, 2021; accepted May 5, 2022

All cells contain specialized signaling pathways that enable adaptation to specific molecular stressors. Yet, whether these pathways are centrally regulated in complex physiological stress states remains unclear. Using genome-scale fitness screening data, we quantified the stress phenotype of 739 cancer cell lines, each representing a unique combination of intrinsic tumor stresses. Integrating dependency and stress perturbation transcriptomic data, we illuminated a network of genes with vital functions spanning diverse stress contexts. Analyses for central regulators of this network nominated C16orf72/HAPSTR1, an evolutionarily ancient gene critical for the fitness of cells reliant on multiple stress response pathways. We found that HAPSTR1 plays a pleiotropic role in cellular stress signaling, functioning to titrate various specialized cell-autonomous and paracrine stress response programs. This function, while dispensable to unstressed cells and nematodes, is essential for resilience in the presence of stressors ranging from DNA damage to starvation and proteotoxicity. Mechanistically, diverse stresses induce HAPSTR1, which encodes a protein expressed as two equally abundant isoforms. Perfectly conserved residues in a domain shared between HAPSTR1 isoforms mediate oligomerization and binding to the ubiquitin ligase HUWE1. We show that HUWE1 is a required cofactor for HAPSTR1 to control stress signaling and that, in turn, HUWE1 feeds back to ubiquitinate and destabilize HAPSTR1. Altogether, we propose that HAPSTR1 is a central rheostat in a network of pathways responsible for cellular adaptability, the modulation of which may have broad utility in human disease.

stress | signaling | network

All living organisms encode cellular stress response systems that enable adaptation to homeostatic insults such as DNA damage, misfolded proteins, and limited oxygen availability (1). These response systems include specialized adaptive pathways, such as the heat shock and hypoxia responses, where misfolded cytosolic proteins and oxygen scarcity (respectively) are sensed and countered with a targeted response. They also include a generalized or integrated stress response (ISR), where kinases sensitive to a variety of stressors phosphorylate eIF2 α to globally remodel protein synthesis (2). Careful titration of the cell's arsenal of stress responses is critical for health, as both insufficient and inappropriate stress signaling cause common diseases (3).

Our understanding of cellular stress adaptation is founded on targeted studies of individual stress response pathways, most of which employ model systems comprising a single stressor in isolation. However, physiological states often represent a complex combination of stresses. For example, cells at the ischemic core of a solid tumor must adapt not only to hypoxia but also to concurrent nutrient starvation and acidosis in a background of cell-intrinsic oncogenic stressors (4). It stands to reason that specialized stress response pathways, commonly coactivated in physiological stress contexts, would not function autonomously in parallel, but rather as an integrated network. However, central mechanisms of oversight linking individual stress response pathways remain elusive.

Here, we leveraged the profound phenotypic heterogeneity of cancer cell lines—each of which faces a unique combination of intrinsic tumor stressors such as aneuploidy, redox state, and biosynthetic demand (4)—as a model system to identify a network of genes with critical functions spanning diverse stress contexts. We identify C16orf72 (HAPSTR1), a deeply conserved, multistress-responsive protein that promotes resilience through simultaneous titration of genotoxic, proteotoxic, nutrient, redox, and paracrine stress response pathways. This function is achieved in cooperation with the E3 ligase HUWE1, which also feeds back to promote HAPSTR1's degradation via ubiquitin-mediated proteolysis. HAPSTR1 is thus central to an integrated network of stress response pathways, where it functionally links intrinsic and environmental stress burdens with network-wide control of stress signaling.

Significance

Cells utilize specialized adaptive pathways to counteract stresses imposed by environmental changes (e.g., nutrient scarcity) or quality control failures (e.g., misfolded proteins). These pathways are commonly coactivated in physiological contexts, but centralized mechanisms linking these pathways have remained elusive. Using a functional genomics approach, we mapped the constituents of and relationships between stress response pathways in human cells. We identified a conserved factor, HAPSTR1, which promotes cellular and organismal resilience under a striking diversity of stress conditions. HAPSTR1, inducible by many stressors, both cooperates with and is degraded by the E3 ligase HUWE1 in a pathway that titrates specialized proteotoxic, genotoxic, nutrient, redox, and paracrine stress response pathways. Thus, HAPSTR1 represents a central coordination mechanism for disease-relevant stress response programs.

The authors declare no competing interest.

This article is a PNAS Direct Submission.

Copyright © 2022 the Author(s). Published by PNAS. This open access article is distributed under Creative Commons Attribution-NonCommercial-NoDerivatives License 4.0 (CC BY-NC-ND).

¹To whom correspondence may be addressed. Email: mendillo@northwestern.edu.

This article contains supporting information online at <http://www.pnas.org/lookup/suppl/doi:10.1073/pnas.2111262119/-/DCSupplemental>.

Published July 1, 2022.

Results

A Molecular Network Controlling Resilience. To identify genes with critical functions in stressed cells, we turned to a panel of 739 diverse cancer cell lines (*SI Appendix*, Fig. S1A) as a model landscape of complex physiological stress states (4, 5). We hypothesized that genetic dependence on stress response master regulators would reflect the stress burden of individual cell lines. If so, we could use a coessentiality approach to identify genes with selective fitness effects in different stress contexts (6, 7). To test this hypothesis, we used genome-scale CRISPR-Cas9 screening data from Project Achilles (5, 8) to quantify the “essentiality”—here, a continuous measure reflecting a gene’s importance for cell fitness—of a panel of 21 stress response master regulators across 739 diverse cancer cell lines (Fig. 1A).

Across cancer cell lines, we found that stress response master regulators were neither universally required nor dispensable for cellular fitness. Rather, these factors demonstrated context-specific essentiality profiles, often reflecting well-known cellular stress phenotypes. For example, the endoplasmic reticulum (ER) stress factor XBP1 was particularly essential in plasma cells, which are characterized by extraordinary protein secretion demands (Fig. 1B) (9). Other examples included the redox factor NFE2L2, which was more essential in cells with high oxidized glutathione; the proteostasis factor HSF1, which was more essential for cells with proteasome mutations; and the hypoxia factor EPAS1 (HIF2 α), which was more essential in clear cell renal cell carcinomas driven by loss of the hypoxia inducible factor alpha (HIF α)—degrading VHL tumor suppressor (Fig. 1C–E). More broadly, dependence on these and other stress response factors was associated with various stress phenotypes predictable from cell line features (*SI Appendix*, Fig. S1B–Q). Thus, genetic reliance upon canonical stress response regulators can provide quantitative insights into the physiological stress phenotype of individual cancer cell lines.

We next sought to use the context-specific fitness effects of stress response master regulators to identify other genes with critical stress response functions. Specifically, we leveraged the concept of coessentiality, which posits that genes important for the same biochemical process tend to have similar patterns of essentiality across biological contexts—in this case, cell lines with specific stress burdens. For example, we hypothesized that cell lines burdened by oxidative stress (and dependent on NFE2L2) would also have heightened dependency on other genes which promote fitness in oxidative stress conditions. Thus, we used FIRWORKS, a bias-corrected, rank-based coessentiality method (10) to identify genes that had essentiality profiles strongly associated with at least two genes in our panel of stress master regulators (*SI Appendix*, Fig. S2A).

Our modified coessentiality approach identified 146 genes with essentiality profiles closely linked with those of known stress response master regulators (*Dataset S1*). These genes encode a functionally diverse group of proteins enriched for stress response and signal transduction (*SI Appendix*, Fig. S2B and C). To better contextualize these 146 genes, we performed RNA sequencing (RNA-seq) to investigate their transcriptional regulation in response to five mechanistically distinct stressors: cyclophosphamide (CPA; genotoxic), CoCl₂ (hypoxic/redox), serum starvation (SS; nutrient), heat shock (HS; proteotoxic), and 2-deoxyglucose (2DG; metabolic/ER stress). Across the transcriptome, 60.0% of all detected transcripts were regulated in response to at least one stressor. Of these stress-responsive genes, 50.7% (4,014 transcripts) were affected by one specific stressor, indicative of regulation by specialized signaling programs (Fig. 1F). Conversely,

16.2% (1,282 transcripts) were regulated by three or more stressors, suggesting that these factors may be part of a more generalized stress response (Fig. 1F). Our set of 146 stress-coessential genes was strongly enriched for these multistress-responsive genes (Fig. 1G and *SI Appendix*, Fig. S2D).

Integration of the coessentiality and transcription profiles of our stress-selective gene set illuminated a global stress response network in human cells (Fig. 1H). Unlike simulated networks constructed from unrelated source nodes, the stress network was densely interconnected, suggesting enrichment for biological signal (*SI Appendix*, Fig. S2E). Indeed, our network demonstrated striking recapitulation of known stress signaling paradigms. We highlight several examples of canonical stress signaling uncovered by our network (Fig. 2A). For example, we observed the critical relationships in oxygen sensing—that is, oxygen tension-specific hydroxylation by EGLN1 and ubiquitin-mediated proteolysis by VHL of HIF α proteins, which otherwise interact with ARNT to transactivate target genes (e.g., DDIT4 for HIF1A). We also observed critical upstream relationships and downstream targets in the oxidative stress, ER stress, ISR, DNA damage response, and nutrient stress signaling pathways (Fig. 2A and *SI Appendix*, *Supplemental Discussion*).

One advantage of coessentiality analysis is the ability to derive insight into which specific genes of a given pathway are most critical for that pathway’s function. For example, critical stress response factors typically regulate a large ensemble of downstream targets. Some of these targets play redundant roles and can be functionally buffered after knockout (KO), resulting in minimal fitness cost across cell lines in a pooled CRISPR screen (11). On the other hand, loss of targets that have roles irreplaceable for pathway function causes a fitness phenotype similar to that of loss of the upstream master regulator—and can thus be identified in coessentiality analyses. As such, the downstream targets identified in our network (e.g., p21/CDKN1A [TP53], TXNRD1 [NFE2L2], and MANF [XBP1]) are likely among the most consequential targets of their pathway. An example of this phenomenon is the ATF4-coessential gene, CEBPG. CEBPG is one of hundreds of ATF4 transcriptional targets, but it also plays a critical role in ATF4 function by heterodimerizing with ATF4 as a required cofactor (12) (Fig. 2A). Another useful feature of our network is that it gives hints as to the driving factors of pathway dependence. As one example, amino acid insufficiency provokes an ISR through EIF2AK4, which is activated by uncharged transfer RNAs (tRNAs) (2). In this pathway module in our network, asparaginyl-tRNA synthetase and asparagine synthetase—unlike synthetases for any other amino acids—are both strikingly coessential with EIF2AK4 and the ISR effector ATF4 (Fig. 2A). This observation, which suggests that asparagine availability is a key determinant of ISR dependence in proliferating cancer cells, is one example of the power of our network in hypothesis generation.

We next considered factors that were coessential with master regulators from more than one stress pathway. We hypothesized that these “crosstalk” genes, located centrally in our network, may represent mechanisms of stress response integration in human cells. Indeed, we found several instances of factors that are known to mediate crosstalk between stress response pathways (Fig. 2B). Examples of crosstalk between specific pathways included MAFK, a hypoxia-inducible protein which acts as a transcriptional cofactor for NFE2L2 (13), thus serving as a mechanism of interplay between hypoxia and oxidative stress signaling (Fig. 2B). We also found proteins with more global roles in stress signaling. For example, TSC2—a negative regulator of mTORC1 activated by diverse stressors (14)—was the single most connected

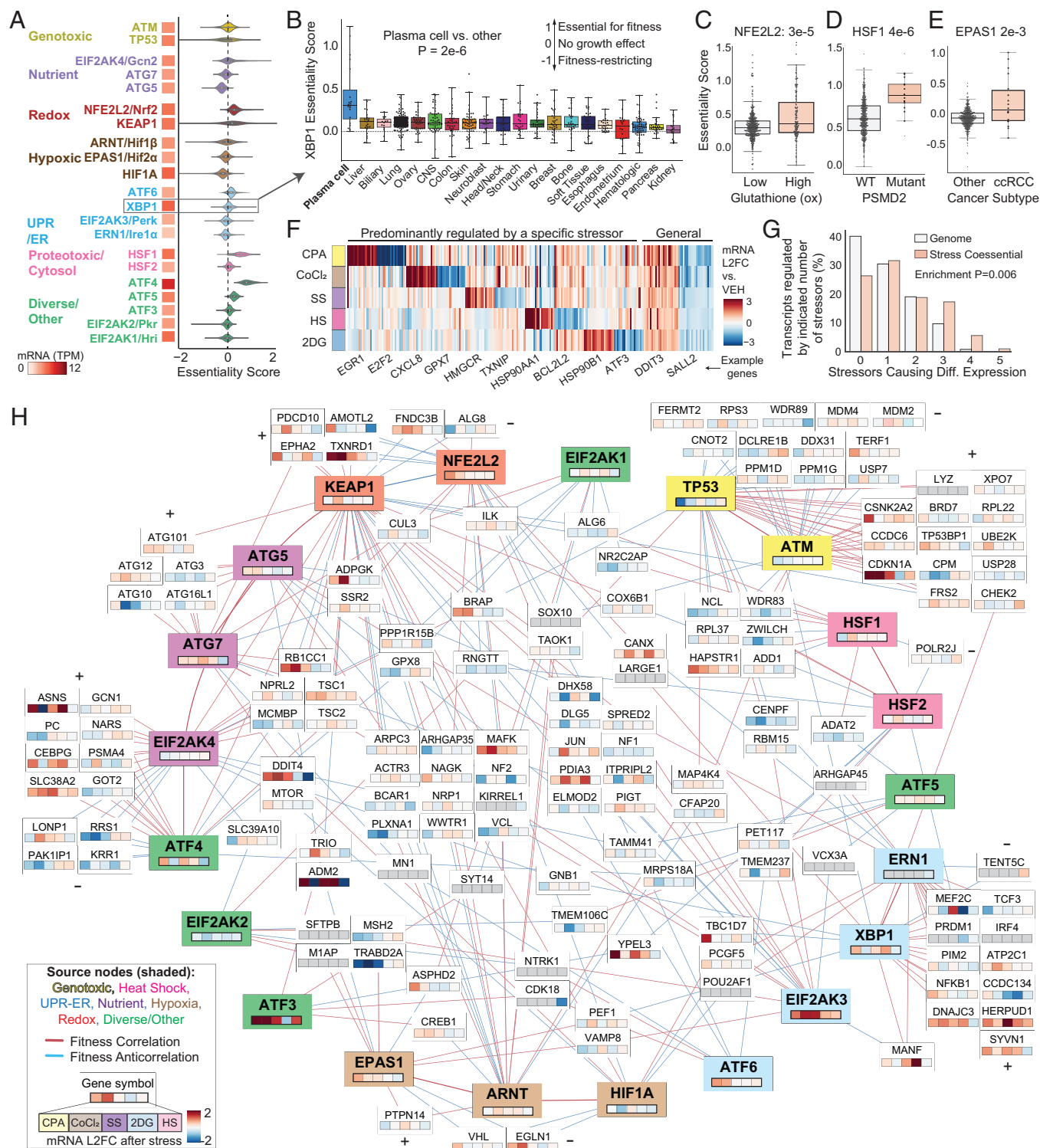


Fig. 1. Deconvolution of cancer stress phenotypes to illuminate a global stress response network in human cells. (A) Essentiality score distributions of master stress response regulators across 739 cancer cell lines. Higher score indicates the gene is more essential for cellular fitness, where 1 is the average of genes considered essential for cell growth. TPM, transcripts per million; CNS, central nervous system. (B) Selective essentiality of ER stress factor XBP1 in secretory plasma cells. Each dot represents a cell line. (C–E) Oxidized (ox) glutathione levels, clear cell renal cell carcinoma (ccRCC) lineage, and proteasome (PSMD2) mutations associated with differential essentiality of oxidative, hypoxic, and proteotoxic master regulators, respectively. More examples in *S1 Appendix*, Fig. S1B–Q. Mann–Whitney *U* test. (F) Specialized and general transcriptional responses to master revealed by transcriptional profiling of MDA-MB-231 cells exposed to five distinct stressors. One example gene labeled per cluster. Log₂ fold change (L2FC) versus vehicle (VEH)/DMSO. CPA, cyclophosphamide; CoCl₂, cobalt chloride; SS, serum starvation; HS, heat shock; 2DG, 2-deoxyglucose. (G) Genes coessential with at least two stress master regulators ($n = 146$) are more likely to be dynamically regulated at the transcript level (differential [Diff.] expression, false discovery rate < 0.01) by acute stress. Two-tailed KS test. Stressors as in F. (H) Integrating stress-transcriptomic data with coessentiality data reveals a global stress response network in human cells. Note legend in lower left. All 21 master regulators in A and 146 stress-coessential genes in G are included. Canonical signaling modules form outside of the network, and crosstalk genes link modules. Positive and negative correlates on exterior of network are grouped and labeled with +/--. Download the network for interactive exploration at <https://mendillolab.org/stressnet>. DMSO, dimethyl sulfoxide; UPR, unfolded protein response.

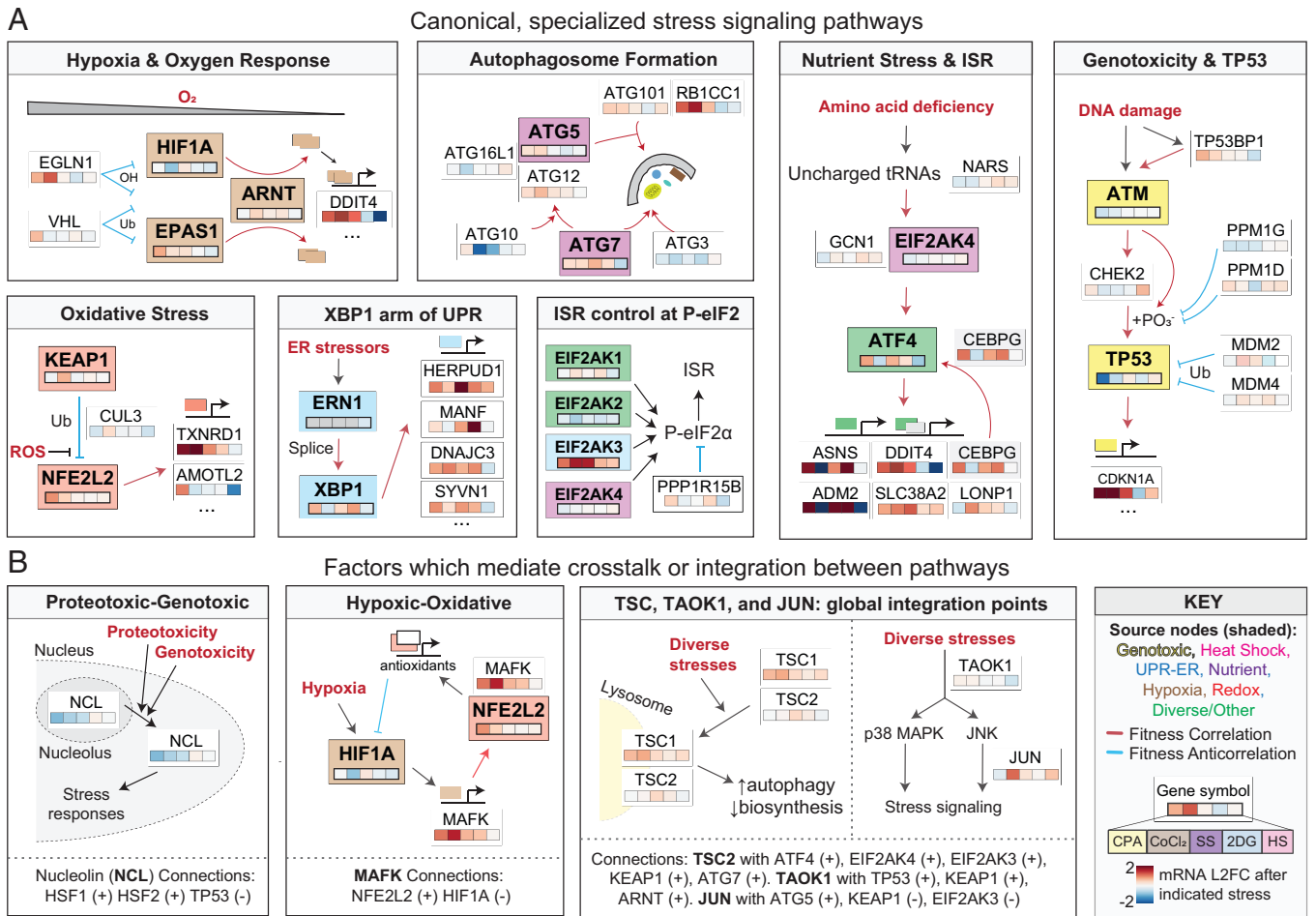


Fig. 2. Example of signaling relationships extracted from the global stress response network. Discussion of each highlighted pathway is present in either the main text or *SI Appendix, Supplemental Discussion*. (A) Examples of upstream regulators and downstream targets of specialized stress response pathways. OH, hydroxyl; Ub, ubiquitin. (B) Examples of crosstalk factors located in the center of the network, which have known roles in the integration of specialized stress responses. CoCl₂, cobalt chloride; L2FC, Log₂ fold change; UPR, unfolded protein response.

gene in the network, with five connections spanning nutrient, oxidative, and ER stress modules (Fig. 2B). TAOK1 and JUN, essential proteins in multistress-responsive protein kinase cascades (15, 16), also displayed connections to several distinct pathways in our network (Fig. 2B).

Altogether, we conclude that our network can offer insights into stress response pathway organization, hierarchy, and regulation in physiological contexts. Importantly, because the source data for our network (fitness screens and transcriptomic experiments) are genome-scale analyses, our network also includes many genes that have no previously described stress response function—or biochemical function in general (*SI Appendix, Fig. S2F*). The striking recapitulation of known biology in our network suggests that these understudied genes may also be important modulators of stress resilience.

The Conserved Protein C16orf72/HAPSTR1 Is a Putative Stress Network Hub. Returning to the question of how cells coordinate their array of specialized stress responses in physiological contexts, we wondered whether any crosstalk genes in our network might serve as novel “hubs” for central coordination of multiple stress response pathways. We reasoned that such genes would be particularly essential to cells concurrently reliant on multiple stress responses—that is, cells facing a combinatorial stress burden. To estimate the combinatorial stress phenotype of individual cell lines, we assessed each cell line’s dependence

(relative to the average cell line) on a master regulator from each network module. We found that certain cell lines were impervious to genetic deletion of all tested master regulators, whereas other lines were concurrently dependent on three or more stress responses (Fig. 3A). For example, HS746T was relatively unaffected by deletion of all tested master regulators, whereas NCI-H2122 was relatively dependent on master regulators from four different stress pathways (Fig. 3A). Of the crosstalk genes in our network, 12 (14%) had essentiality profiles that increased in a dose-responsive fashion with the combinatorial stress burden (number of concurrent stress dependencies) of the cell line (*Dataset S1*). These 12 genes included known poly-stress factors such as TAOK1 (15) and NCL (17). We further queried this list for genes that were induced by multiple stressors, reasoning that this orthogonal criterion—while not necessary for a gene to have important stress response functions—would increase our likelihood of identifying a factor causally related to global stress signaling (Fig. 3B). Altogether, this approach nominated one factor, C16orf72, a gene of unknown function that we renamed HAPSTR1 (**H**UWE1-**A**ssociated **P**rotein modifying **S**Tress **R**esponses) for reasons described below.

HAPSTR1, encoded across a 30-kb stretch of chromosome 16, is a predicted protein-coding gene with no known biochemical function. HAPSTR1 is conserved through yeast and certain plants (Fig. 3C), with a particularly conserved region that has been classified by the Protein Families Database

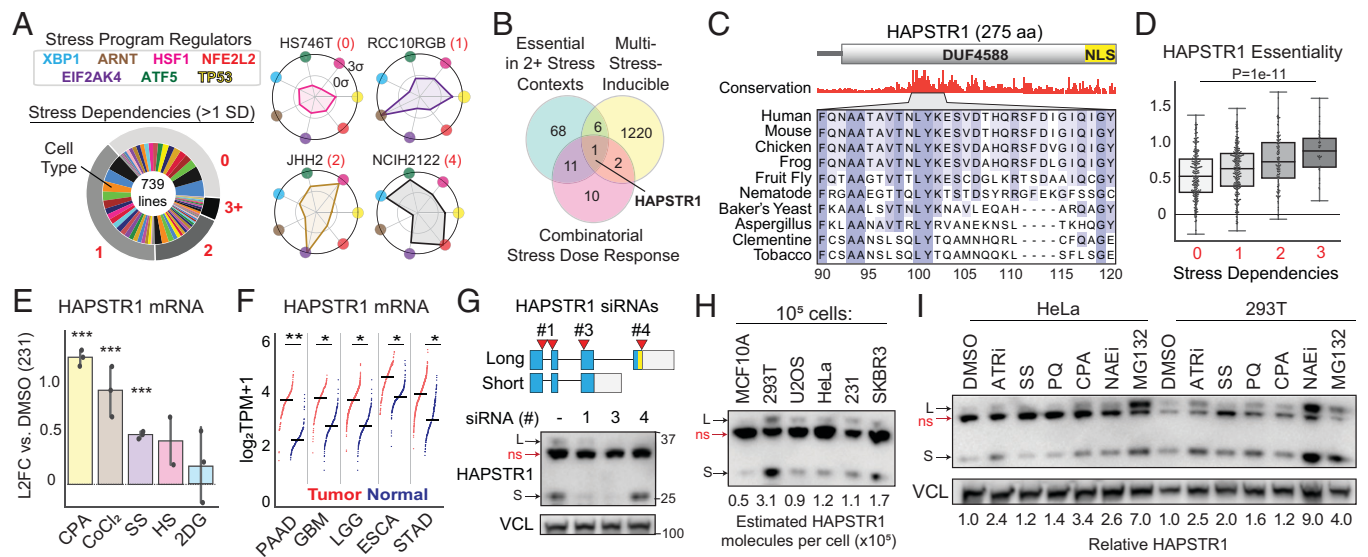


Fig. 3. Analysis of putative stress network hubs identifies the conserved and multistress-inducible protein C16orf72/HAPSTR1. (A) The stress phenotype of cancer cells reflected in relative essentiality of the indicated stress response master regulators. Example cell lines on *Right*. Polar graph radius indicates the line's relative dependence on the indicated stress response factors (versus average cell line). Range -3 to $+3$ SDs. Project Achilles data. (B) Filtering the stress network for genes with central hub characteristics (essential in 2+ stress contexts from Fig. 1H; multistress inducible based on transcription in 1 h and combinatorial stress dose-response based on A nominates C16orf72/HAPSTR1. (C) HAPSTR1 contains a conserved domain of unknown function (DUF4588), including a particularly conserved region (highlighted), as well as a C-terminal NLS. (D) HAPSTR1 essentiality increases with the number of stress dependencies of a given cell line, as in A. Pearson P value. (E) HAPSTR1 induction by stress (MDA-MB-231). CPA, 100 μ M; SS, 0% FBS; HS, 42°C \times 1 h; 2DG: 10 mM. RNA-seq, ***FDR < 0.005. Mean \pm SEM. (F) HAPSTR1 overexpression in tumors versus matched normal tissue (multivariate ANOVA). PAAD, pancreatic adenocarcinoma; GBM, glioblastoma; LGG, low-grade glioma; ESCA, esophageal carcinoma; STAD, stomach adenocarcinoma. **FDR < 0.005, *FDR < 0.05. Data from GEPIA2. (G) siRNAs targeting one or both HAPSTR1 isoforms validate the protein expression of two HAPSTR1 isoforms (long [L] and short [S]). ns, nonspecific. Immunoblot, 293T. (H) Estimated HAPSTR1 protein abundance (both isoforms) in nontumorigenic (MCF10A) and tumorigenic (all other) cell lines (*SI Appendix, Fig. S5 A–D*). (I) Stress-dynamics of HAPSTR1 protein. Representative of $n > 3$; 16-h treatments: ATRI, AZD6738 1 μ M; SS, 0% serum; PQ, paraquat 1 μ M; CPA, 100 μ M; NAEi, MLN4924 500 nM; MG132, 1 μ M. CoCl₂, cobalt chloride 250 μ M; DMSO, dimethyl sulfoxide; L2FC, Log₂ fold change.

(PFAM) as the domain of unknown function DUF4588 (18). Sequence analysis and structural predictions for HAPSTR1 highlighted a motif of two tandem amphipathic helices (beginning at residues 59 and 86), a disordered stretch (beginning around residue 150), and a C-terminal nuclear localization signal (NLS; residues 252 to 275) (Fig. 3C and *SI Appendix, Fig. S3A–C*). Per our selection criteria, HAPSTR1—linking proteotoxic and genotoxic modules in our network—was particularly important to the fitness of cancer cells characterized by a combinatorial stress burden (Fig. 3D). This finding was reproducible using data from an orthogonal large-scale screening project with different technical parameters (*SI Appendix, Fig. S4A and B*) (19). Considering stress-induction, HAPSTR1 messenger RNA (mRNA) was induced by genotoxic, hypoxic, and nutrient stressors in our transcriptomic experiments (Fig. 3E). Published datasets indicate that regulation of HAPSTR1 transcription by diverse stressors is conserved in *Caenorhabditis elegans* and budding yeast (*SI Appendix, Supplemental Discussion*). Consistent with transcriptional regulation by changing stress environments, HAPSTR1 expression—though ubiquitous across tissues—is dynamic through development in humans and mammalian model organisms (*SI Appendix, Fig. S4C and D*). HAPSTR1 mRNA is also frequently higher in tumors than in matched normal tissue in a manner associated with tumor aggression (Fig. 3F and *SI Appendix, Fig. S4E and F*).

We next investigated the protein encoded by HAPSTR1, first purifying HAPSTR1 fused to maltose-binding protein (MBP) to validate our antibody and facilitate immunoblot quantitation (*SI Appendix, Fig. S5 A–D*). From transcriptomic studies, HAPSTR1 has two predicted isoforms: a long isoform comprising all four exons and a short isoform comprising the first three exons, with predicted molecular weights of 31 and 23 kDa, respectively (Fig. 3G). HAPSTR1 immunoblots produced three bands of

~ 32 , 30, and 23 kDa. CRISPR-Cas9 KO and isoform-specific small interfering RNAs (siRNAs) indicated that the 32- and 23-kDa species represent HAPSTR1's two isoforms, whereas the 30-kDa band is nonspecific (Fig. 3G and *SI Appendix, Fig. S5E*). Consistent with our transcription data, HAPSTR1 was dynamically regulated at the protein level. HAPSTR1 expression was lowest in the only nontumorigenic line assayed (MCF10A), highest in the most HAPSTR1-dependent lines (SKBR3, 293T), and inducible by exogenous stressors (Fig. 3H and I). There were no apparent differences in the relative abundance of the long and short isoforms across different cell lines and stress conditions. Notably, HAPSTR1 exon four (long isoform specific) contains the predicted NLS. We validated that deletion of this NLS attenuated nuclear localization of overexpressed full-length HAPSTR1 (*SI Appendix, Fig. S5F and G*). Notably, however, both long and short HAPSTR1 isoforms can access the nuclear as well as cytoplasmic compartments (*SI Appendix, Fig. S5H–K*; versus the non-specific 30-kDa species, which is purely cytoplasmic). Altogether, we found that the putative stress network hub gene HAPSTR1 encodes an evolutionarily conserved, multistress-responsive, mixed cytoplasmic and nuclear protein with two primary isoforms.

HAPSTR1 Empowers Resilience to Diverse Stressors In Vitro and In Vivo. We reasoned that if HAPSTR1 is truly central to a global stress response network, HAPSTR1 depletion would cause signaling alterations spanning distinct stress response pathways. Thus, we first assessed the transcriptional consequence of HAPSTR1 depletion using an siRNA pool targeting both isoforms in a panel of breast cancer cell lines with varying degrees of dependence on HAPSTR1 (low dependence, MDA-MB-231; moderate dependence, ZR-75-1; high dependence, SK-BR3) (*SI Appendix, Fig. S6A and B*). Across cell lines,

HAPSTR1 knockdown increased expression of DNA damage response genes while decreasing inflammatory, hypoxic, redox, and other stress response genes (Fig. 4A). The observation that HAPSTR1 regulates key factors in many different stress response pathways was exquisitely consistent across experiments performed with three independent siRNAs (SI Appendix, Fig. S6C–F). It is notable that HAPSTR1 remodeled stress signaling even in MDA-MB-231 cells, which do not depend on HAPSTR1 for growth in standard culture conditions (SI Appendix, Fig. S6A and B). Together, these data suggest that HAPSTR1 has a far-reaching stress network function, active in all cells but with different fitness implications depending on intrinsic or environmental stress burden.

To directly test the hypothesis that HAPSTR1 becomes critical for fitness in the presence of stress, we designed a targeted screen to test the growth of HAPSTR1-depleted cells after exposure to a diverse panel of stressors. Strikingly, even in cells where HAPSTR1 is not essential for growth at baseline, HAPSTR1 loss dramatically and acutely reduced resilience to nearly every stressor tested, including redox, genotoxic, and nutrient stress perturbations (Fig. 4B and C and SI Appendix, Fig. S6G and H). These data support the inference from cancer cell line modeling that HAPSTR1 dependence is tightly linked with cellular stress burden. Moreover, these data comport with recent genome-scale fitness screens in which HAPSTR1 scored among the most critical

determinants of adaptability to redox, genotoxic, proteotoxic, and infectious stressors (Fig. 4D) (20–25). Thus, HAPSTR1 critically regulates cellular resilience in diverse contexts in vitro.

We next investigated whether HAPSTR1's role in cellular stress tolerance has implications for organismal resilience in vivo. We generated a *C. elegans* KO strain of the HAPSTR1 ortholog, haps-1 (henceforth, haps-1; SI Appendix, Fig. S6I and J). In basal conditions, similar to wild-type (WT) nematodes, HAPSTR1-deficient animals were viable and appropriately sized and produced healthy offspring (Fig. 4E and F). However, HAPSTR1/haps-1 KO animals were unable to withstand, recover from, or reproduce normally during exposure to distinct stressors, including paraquat (redox stress), neddylation inhibition (multiple stress phenotypes including proteotoxicity), or camptothecin (genotoxic stress) (Fig. 4 G–J and SI Appendix, Fig. S6J). We note that HAPSTR1/haps-1 promoted resilience in both proliferating germline and postmitotic tissues, indicating that HAPSTR1's regulation of stress responses spans tissue type and differentiation stages. Further supporting the conservation of HAPSTR1's stress response function, published yeast screens indicate that HAPSTR1 promotes resilience to thermal, oxidative, disulfide, and nutrient stressors as well as antibiotics (SI Appendix, Supplementary Discussion). Thus, the stress-inducible protein HAPSTR1 is a critical and evolutionarily conserved mediator of multistress resilience in vitro and in vivo.

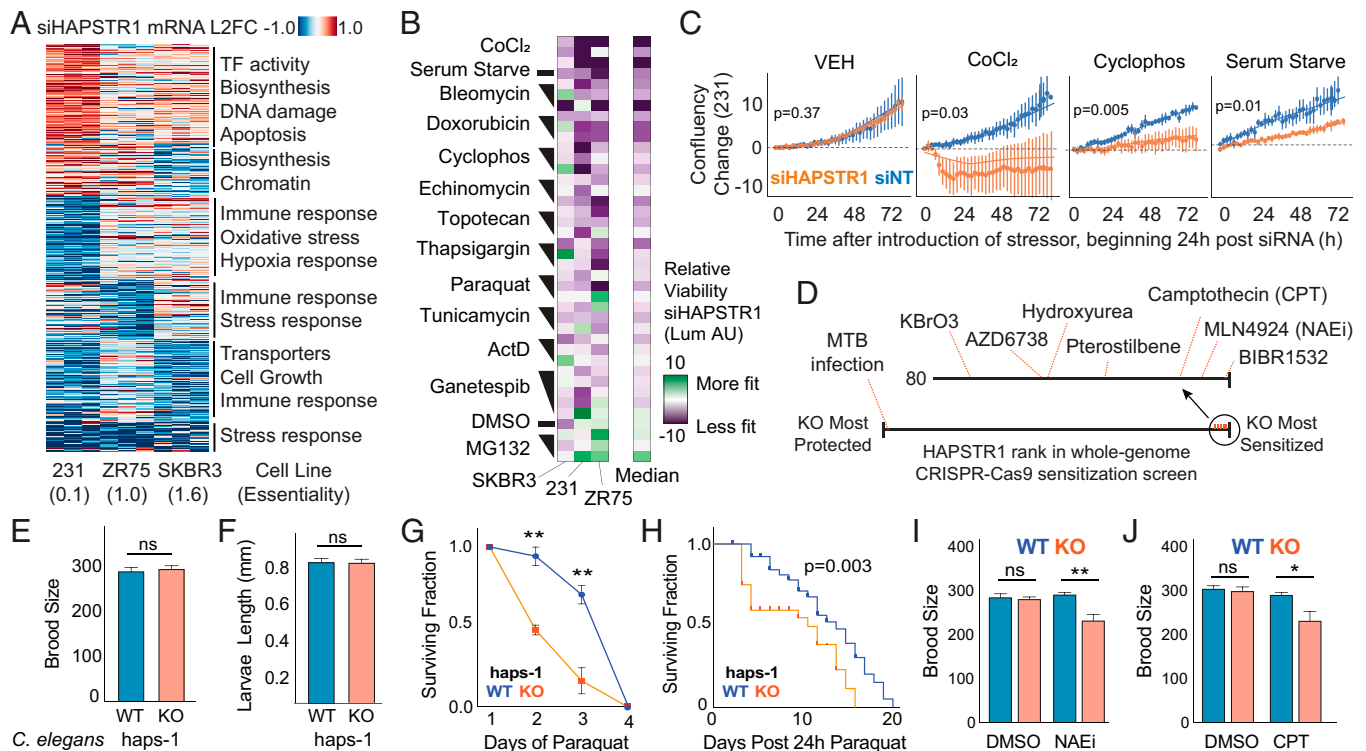


Fig. 4. HAPSTR1 confers resilience to diverse stressors in vitro and in vivo. (A) Transcriptomic consequences of HAPSTR1 siRNA (siHAPSTR1), log₂ fold change (L2FC) vs. nontargeting control siRNA (siNT), in three cell lines with varying HAPSTR1 essentiality scores (shown below line name; SI Appendix, Fig. S6A and B). Gene set enrichment analysis terms (false discovery rate < 1e-5) are highlighted in each cluster. K-means, K = 6. Any gene differentially expressed in any line included. (B) HAPSTR1 confers multistress resilience to breast cancer cells. Viability assessed by CellTiterGlo Luminescence in arbitrary units (Lum AU). Drugs sorted by mean effect difference across doses. ActD, actinomycin D. (C) Live cell imaging traces of WT and HAPSTR1-depleted cells after exposure to stressors; n = 3, two-tailed t test of area under curve values. CoCl₂, 250 μM, redox stress; cyclophosphamide, 50 μM, genotoxic stress; SS, 0% serum, nutrient and ER stress. (D) HAPSTR1 is a hit in many recent whole-genome CRISPR-Cas9 sensitization screens (20–25). Bottom line indicates genome-wide ranked list of genes whose loss protects (KO Most Protected; left of line) to genes whose loss sensitizes (KO Most Sensitized; right of line) in a particular screen condition. The rank of HAPSTR1 in each screening condition is indicated. That is, HAPSTR1 loss sensitizes cells to most stressors/agents shown but promotes fitness in the context of *Mycobacterium tuberculosis* (MTB) infection. (E and F) Normal reproduction and size of HAPSTR1/haps-1 KO *C. elegans*. (G–J) haps-1 KO nematodes have reduced survival, adaptability, and reproductive success after exposure to stressors. Log-rank (H) or two-tailed t test. *P < 0.05, **P < 0.01; ns: not significant (P ≥ 0.05). CPT, camptothecin 70 μM × 6 h. NAEi: MLN4924, 100 μM × 24 h. Paraquat, 8 mM × duration indicated. CoCl₂, cobalt chloride; Cyclophos, cyclophosphamide; DMSO, dimethyl sulfoxide (VEH); L2FC, Log₂ fold change. Error bars represent SEM.

HAPSTR1 Titrates Cell-Autonomous and Paracrine Stress Signaling. HAPSTR1's proresilience function and broad regulation of stress response gene expression in unperturbed cell lines led us to further investigate the role of HAPSTR1 in the adaptive signaling response to acute stressors. We first leveraged stress program reporter proteins and targeted stress perturbations (Fig. 5*A* and *SI Appendix*, Fig. S7*A*). Consistent with a role for HAPSTR1 in combating cancer cell-intrinsic stresses, in the absence of exogenous stress HAPSTR1 loss induced a stress response including up-regulation of the DNA damage marker γ H2AX, the autophagy protein LC3-II, the ER chaperone HSPA5 (BiP), the general stress factor ATF3, and the tumor suppressor TP53 (Fig. 5*A*). HAPSTR1's role in the adaptive changes induced by stress was also profound. For example, across stress environments, HAPSTR1 was required for the induction of the critical cytosolic chaperone HSP70/HSPA1A and for suppression of a TP53 and p21/CDKN1A response (Fig. 5*A*). It is worth noting that consistent with transcriptomic findings (*SI Appendix*, Fig. S6*F*), depletion of HAPSTR1's full-length isoform via siRNA-4 was sufficient to entirely abrogate HAPSTR1's effects on signaling (Fig. 5*A*).

To assess the role of HAPSTR1 in stress signaling more broadly, we employed unbiased transcriptomics in combination with three distinct stress perturbations. The effects of HAPSTR1 loss on the transcriptional adaptation to stress were striking. For example, 2,780 genes (25.7% of detected transcripts) were differentially expressed in serum-starved cells without HAPSTR1 compared to starved cells with HAPSTR1 (Fig. 5*B*). Consistent with protein-level data, HAPSTR1 titrated the specialized canonical signaling response to individual stressors, specifically altering metabolism and lysosome genes with SS, replication stress genes with CPA, and oxygen response genes with CoCl_2 (Fig. 5*B–E*). These stressor-specific alterations—for example, failure to induce the antioxidant SOD2 in HAPSTR1-depleted cells under redox stress conditions, but equivalent expression at baseline and after other stresses—suggest that HAPSTR1 oversees the execution of specialized responses activated by specific stressors. HAPSTR1 loss also regulated noncanonical stress responses provoked by each stress (e.g., preventing the increase in hypoxia signaling provoked by SS) (Fig. 5*B*). Thus, HAPSTR1 simultaneously regulates the multiple specialized pathways—both classical and auxiliary—induced by physiological stressors.

Across all stresses, we noticed that secreted chemokines and paracrine signaling factors were markedly induced at the transcript level in WT but not HAPSTR1-depleted cells (Fig. 5*B–D* and *F*). Chemokine arrays in two cell lines confirmed that many proteins typically up-regulated and secreted during stress—for example, interleukin (IL)-6 and several colony-stimulating factors—were less abundant in conditioned media from cells lacking HAPSTR1 (Fig. 5*G* and *H* and *SI Appendix*, Fig. S7*B* and *C*). Decreased chemokine secretion may relate to reduced chemokine synthesis, reduced secretion activity, or both (i.e., muted feedforward signaling). While the transcriptomic evidence indicated that HAPSTR1 robustly regulates chemokine synthesis, not all chemokines reduced in HAPSTR1-depleted media were regulated by HAPSTR1 transcriptionally (e.g., angiogenin; *SI Appendix*, Fig. S7*D*). To test whether HAPSTR1 also regulates chemokine secretion more directly, we leveraged a model chemokine: cyclophilin A (PPIA). This chemokine, when ectopically expressed at high levels, is efficiently secreted in a manner blocked by inhibitors of its vesicular secretion pathway (*SI Appendix*, Fig. S7*E*) (26). We found that HAPSTR1 depletion dramatically reduced the secretion of exogenous PPIA-FLAG, resulting in intracellular accumulation (Fig. 5*J*). Thus, in

addition to promoting synthesis of various stress-responsive chemokines, HAPSTR1 appears to regulate a pathway by which certain chemokines are released. Intercellular stress signaling via paracrine factors is critical in contexts such as fetal development, tumor-microenvironment crosstalk, and wound healing (3). Fittingly, conditioned media from HAPSTR1-depleted cells had a reduced ability to promote migration of cancer cells across a scratch wound (Fig. 5*J*). Altogether, these data suggest that HAPSTR1 is deeply intertwined in the regulatory network of a diverse set of specialized stress response pathways, both cell autonomous and paracrine in nature.

A Conserved Interaction between HAPSTR1 and HUWE1 Governs HAPSTR1 Stability. To better understand how HAPSTR1 achieves such broad regulation of stress signaling, we performed immunoprecipitation coupled with mass spectrometry (IP-MS) to identify proteins that interact with full-length HAPSTR1 in cells (Fig. 6*A* and *Dataset S2*). By far, the most enriched interacting protein was HUWE1, a HECT E3 ligase with a pleiotropic array of substrates from major cell-fate determination pathways (31). Confirming the physical interaction, we reciprocally coimmunoprecipitated endogenous HUWE1 and FLAG-HAPSTR1 (Fig. 6*B*). Furthermore, purified MBP-HAPSTR1 but not MBP alone efficiently isolated HUWE1 from cell lysates (Fig. 6*C*). We found no evidence that stress modified the affinity of the HAPSTR1–HUWE1 interaction or the proportion of HAPSTR1 bound to HUWE1 (*SI Appendix*, Fig. S8*A* and *B*). Notably, the interaction between HAPSTR1 and HUWE1 is evolutionarily conserved, as the yeast HAPSTR1 ortholog (YJR056C) was the strongest interacting partner for TOM1 (HUWE1) in a recent proteomic experiment (Fig. 6*D*) (27).

We noticed that endogenous HUWE1 immunoprecipitations copurified long (275–amino acids [aa]) and short (198-aa) HAPSTR1 isoforms equivalently (Fig. 6*E*). To confirm that both HAPSTR1 isoforms directly interact with HUWE1, we knocked down endogenous HAPSTR1 before expressing one or both isoforms with different tags. Indeed, both isoforms were able to copurify HUWE1 (Fig. 6*F*). Intriguingly, from this design we were able to observe oligomerization of the two isoforms (Fig. 6*F*), a finding consistent with our gel filtration experiments, which consistently demonstrated tight coelution of recombinant full-length and C-terminal-truncated HAPSTR1 proteins (*SI Appendix*, Fig. S5*A–C*). The latter observation suggested that an oligomerization interface exists somewhere within HAPSTR1's first 160 aa (*SI Appendix*, Fig. S5*C*).

To directly search for putative domains within HAPSTR1 that mediate oligomerization and/or HUWE1 binding, we performed a series of coimmunoprecipitation experiments with truncated HAPSTR1 fragments. We also tested point mutants of four residues (F90, A94, Y101, and G119) perfectly conserved across all HAPSTR1 orthologs (Fig. 3*C* and *SI Appendix*, Fig. S3*B* and *C*). For these mutants, small uncharged residues (alanine/glycine) were mutated to a large, charged residue (arginine), with all other residues exchanged for alanine. First, considering oligomerization, we found that all constructs containing the 80 to 152 region of HAPSTR1 oligomerized *in vivo* (Fig. 6*G* and *SI Appendix*, Fig. S8*C*). This region, which we now term the HBO domain (HUWE1-binding and HAPSTR1 Oligomerization), also contained the four perfectly conserved residues we mutagenized. Mutation of one of these residues, G119, was sufficient to block oligomerization (Fig. 6*G–H*). Adapting the AlphaFold2 algorithm (28), we predicted the structure of oligomeric HAPSTR1, first observing that dimers were considered by the model to be more favorable than higher order oligomers (*SI Appendix*, Fig. S8*D*). Remarkably

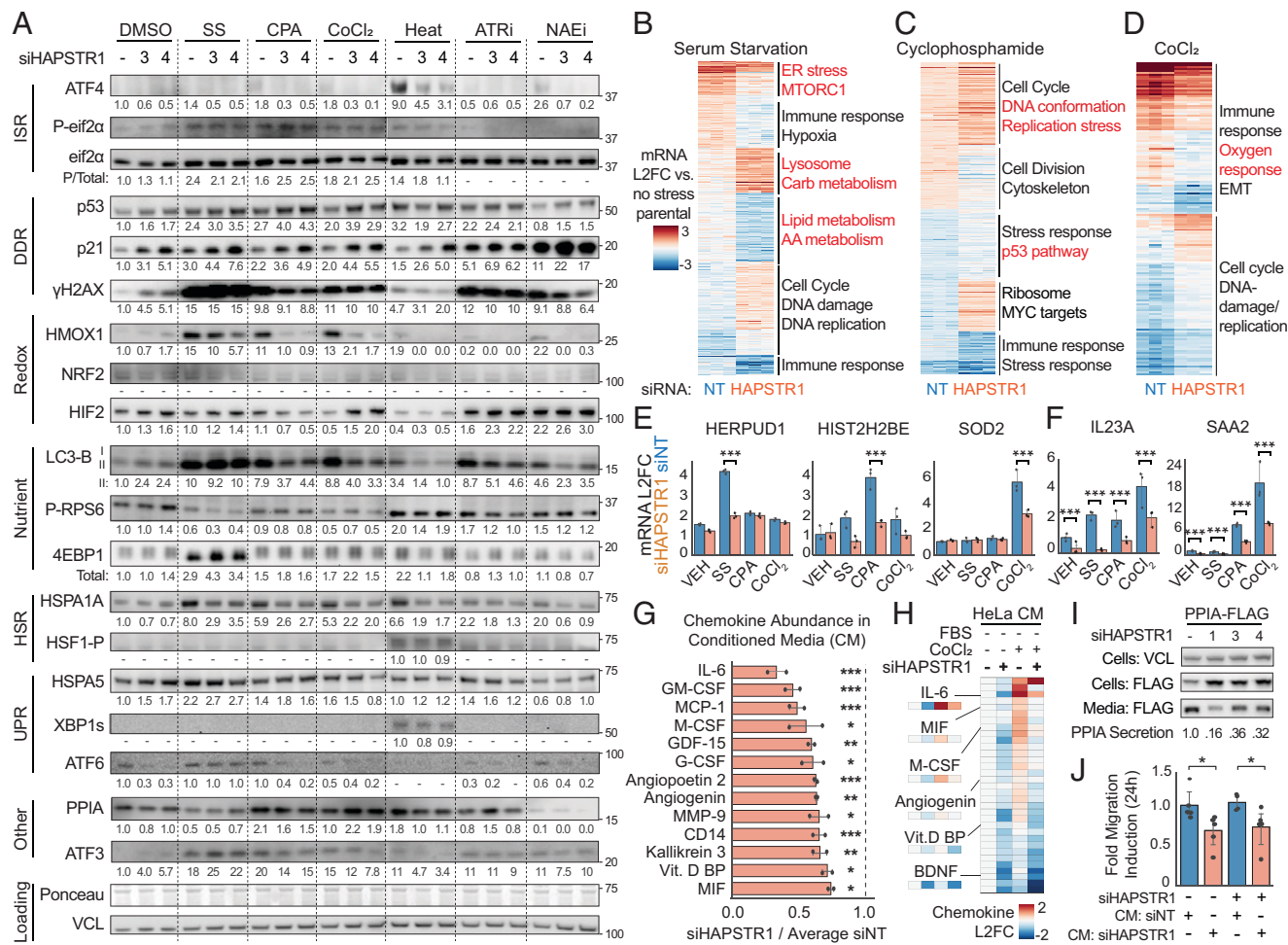


Fig. 5. HAPSTR1 oversees cell-autonomous and paracrine stress signaling. (A) Effect of HAPSTR1 depletion on canonical stress response proteins in different stress contexts. Note: HAPSTR1 siRNA (siHAPSTR1) #3 depletes long and short HAPSTR1 isoforms, whereas #4 depletes only the long isoform. U2OS. After 48 h of siRNA, 16-h drug treatments. SS, 0% FBS; CPA, 100 μ M; Heat, 43C \times 2 h; CoCl₂, (cobalt chloride 250 μ M); ATRi, AZD6738 1 μ M; NAEI, MLN4924 500 nM. Blots sliced between CoCl₂ and Heat to facilitate antibody incubation but are the same gel/membrane/image exposure. Pathways (Left): ISR, DDR, DNA damage response; UPR, unfolded protein response. Relative quantitation shown, with “-” indicated where no confident band could be detected even at high exposures. (B–D) HAPSTR1 depletion rewires the transcriptomic response to three stressors. MDA-MB-231. Red text: stressor-specific changes. Data normalized to “nonstressed” nontargeting siRNA (siNT) and vehical (DMSO; VEH). I.e., the siNT samples [leftmost columns in each heatmap] indicate the “normal” response of the gene to that stressor. Gene set enrichment analysis terms indicated enriched at false discovery rate < 1e-5. AA, amino acid; carb, carbohydrate; EMT, epithelial to mesenchymal transition. (E and F) Examples of stressor-specific cell-autonomous (E) and broadly regulated chemokine (F) transcripts. ***FDR < 1e-5. (G and H) Chemokine abundance in conditioned media from HAPSTR1-depleted MDA-MB-231 (G) or HeLa (H) as quantified by array. All cells kept in serum-free media for 36 h, with indicated HeLa cells also treated with CoCl₂, 250 μ M. FBS, fetal bovine serum. (I) Transient transfection of the model chemokine PPIA-FLAG causes its secretion in WT but not HAPSTR1-depleted HeLa cell. (J) Effect of conditioned media (CM) from WT or HAPSTR1-depleted cells on the migration of cells across a scratch wound in serum-free media, MDA-MB-231; two-tailed test, *P < 0.05, **P < 0.01, ***P < 0.005. DMSO, dimethyl sulfoxide; IL, interleukin; L2FC, Log₂ fold change. Bar graphs are mean \pm SEM.

consistent with our experimental data, the dimeric HAPSTR1 model aligned the two proteins along a symmetric interaction interface composed of each isoform’s HBO domain helix, with the G119 residue (experimentally required for oligomerization) positioned at the closest contact site in this interface (Fig. 6J). Compared with the other point mutants, we found that G119R HAPSTR1 was relatively unstable and subject to rapid proteasomal degradation (SI Appendix, Fig. S8E and F), raising the possibility that oligomerization promotes HAPSTR1 stability.

Next, considering HUWE1 binding, we found that HAPSTR1 fragments smaller than the short isoform did not efficiently bind HUWE1 (Fig. 6G and SI Appendix, Fig. S8C). Strikingly, however, mutagenesis of any of the perfectly conserved HAPSTR1 residues was sufficient to prevent (F90A, A94R, Y101A) or reduce (G119R) HUWE1 binding (Fig. 6G and H). These data suggest that the function of the tightly conserved motif within HAPSTR1’s HBO domain (Fig. 3C) is to mediate the conserved interaction between HAPSTR1 and HUWE1. Finally, we performed reciprocal

domain experiments using HUWE1 fragments, which revealed a HAPSTR1-binding region on HUWE1 (residues 2,365 to 3,090; Fig. 6J and SI Appendix, Fig. S8G). This region is poorly resolved in existing HUWE1 structures but is known to contain a “tower” motif and several ubiquitin-binding motifs (30).

We next investigated the functional significance of the HAPSTR1–HUWE1 interaction. Given that HUWE1 is a ubiquitin ligase, we tested whether HUWE1 promotes HAPSTR1 ubiquitination or degradation. Indeed, we found that HUWE1 depletion, despite not affecting HAPSTR1 mRNA levels, markedly increased HAPSTR1 protein abundance (Fig. 6K and L). This increase corresponded to heightened stability of HAPSTR1, with HUWE1 depletion raising the half-life of this short-lived protein from ~84 min to 189 min (Fig. 6L and M). Consistent with HUWE1’s ability to directly interact with both HAPSTR1 isoforms, HUWE1 destabilized HAPSTR1’s long and short isoforms equally (Fig. 6L). Proteasome inhibition prevented HAPSTR1 clearance by HUWE1, indicating that HUWE1 promotes HAPSTR1’s

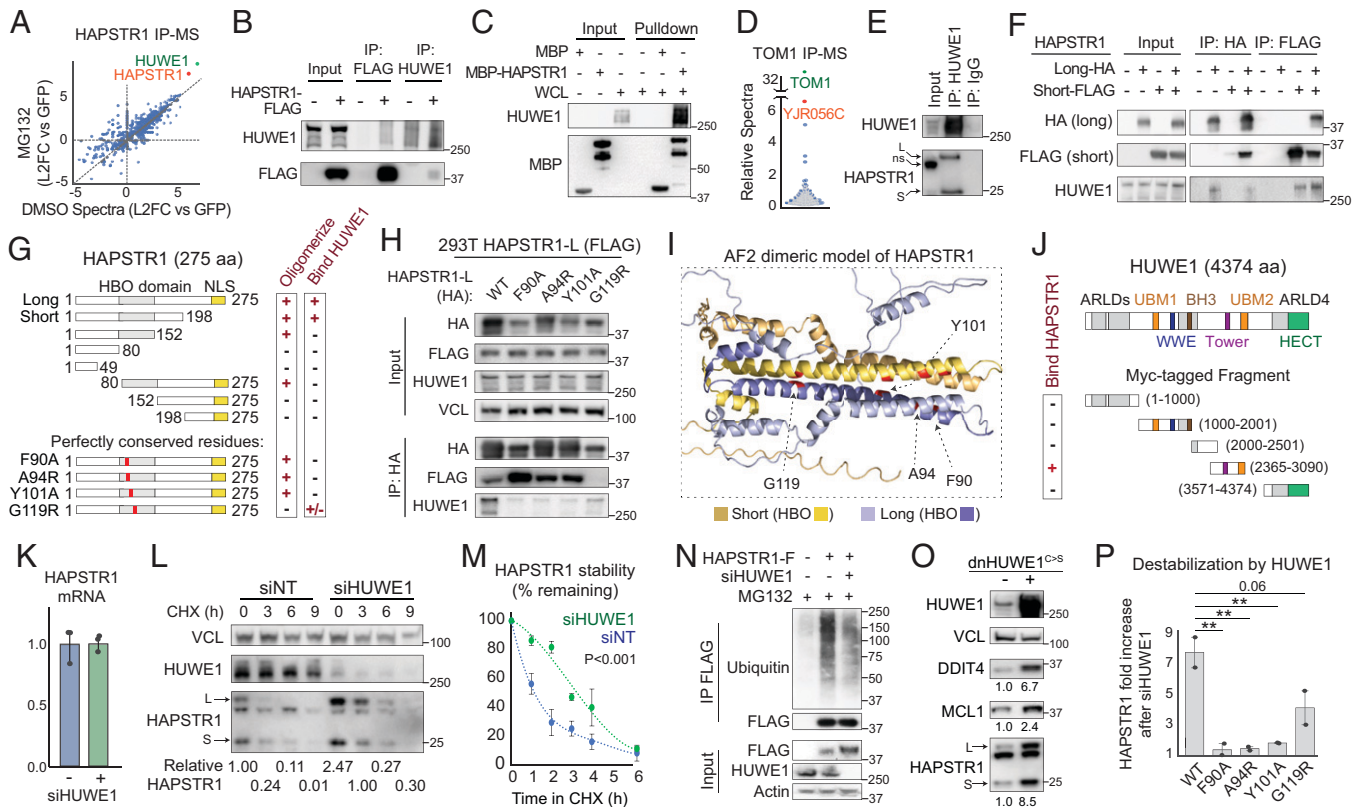


Fig. 6. A conserved interaction between HAPSTR1 and HUWE1 promotes HAPSTR1 polyubiquitination and degradation. (A) HUWE1 is the dominant HAPSTR1 interacting protein by IP-MS in nonstress (DMSO) and stress (proteasome inhibitor MG132, 5 μ M \times 6 h) contexts. (B) Reciprocal coimmunoprecipitation (co-IP) of endogenous HUWE1 and HAPSTR1-FLAG. (C) Purified MBP-HAPSTR1 isolates HUWE1 from HeLa whole cell lysates (WCL). (D) HAPSTR1's yeast ortholog, YJR056C, was found to be the top interacting partner for yeast HUWE1/TOM1 in a recent proteomic study (27). (E) Endogenous HUWE1 co-IPs are enriched for endogenous HAPSTR1 long (L) and short (S) isoforms but not the nonspecific (ns) species recognized on input immunoblots. (F) Long and short HAPSTR1 isoform co-IPs demonstrate that both can independently bind HUWE1 and that the isoforms can oligomerize. 293T, transient transfections. (G) HAPSTR1 domain mapping experiments summarized (SI Appendix, Fig. S8). Domains and mutated residues color highlighted. (H) Highly conserved residues within HAPSTR1 mediate HUWE1 binding and oligomerization. 293T. L, long isoform. (I) Predicted structure of HAPSTR1 as a dimer using AlphaFold2 (28, 29). Key residues highlighted. Note that certain disordered/low-confidence regions (represented by stringlike appearance) continue just out of frame (SI Appendix, Fig. S8D). (J) Domain schematic of HUWE1 (30) and identification of a HAPSTR1-binding interface on HUWE1 by reciprocal co-IP (SI Appendix, Fig. S8). (K) HUWE1 siRNA (siHUWE1) does not control HAPSTR1 mRNA. (L) HUWE1 destabilizes HAPSTR1 protein. Representative experiment of $n > 3$. CHX, cycloheximide 40 μ g/mL. (M), Quantification of HAPSTR1 stability in cells with or without HUWE1. (N) HUWE1 promotes ubiquitination of HAPSTR1-FLAG (HAPSTR1-F) in vivo. Denaturing co-IP, 10 μ M MG132 \times 6 h, 293T. (O) Transient expression of active site mutant (C4341S; dnHUWE1), stabilizing canonical substrates such as MCL1 and DDIT4 (Fig. 6O). Suggesting that the HUWE1 E3 ligase is directly responsible for HAPSTR1 ubiquitination, we found that dnHUWE1 profoundly increased HAPSTR1 abundance (Fig. 6O). Further demonstrating a direct role for HUWE1 in HAPSTR1 degradation, we found that HUWE1-binding-deficient HAPSTR1 point mutants were protected from HUWE1-mediated destabilization (Fig. 6P and SI Appendix, Fig. S8J). Altogether, these data indicate that an exquisitely conserved interaction interface shared among HAPSTR1 isoforms mediates binding to HUWE1, which then promotes HAPSTR1 degradation through K48 polyubiquitination.

proteasomal degradation (SI Appendix, Fig. S8H). Fittingly, we found that HAPSTR1 polyubiquitination is reduced in vivo after HUWE1 depletion (Fig. 6M). Ubiquitin linkage-specific antibodies suggest that the HUWE1-dependent ubiquitin chains on HAPSTR1 are K48 and not K63 linked (SI Appendix, Fig. S8I). As has been observed for several other E3 ligases, we found that overexpression of the catalytically inactive mutant HUWE1 resulted in a dominant negative effect (C4341S; dnHUWE1), stabilizing canonical substrates such as MCL1 and DDIT4 (Fig. 6O). Suggesting that the HUWE1 E3 ligase is directly responsible for HAPSTR1 ubiquitination, we found that dnHUWE1 profoundly increased HAPSTR1 abundance (Fig. 6O). Further demonstrating a direct role for HUWE1 in HAPSTR1 degradation, we found that HUWE1-binding-deficient HAPSTR1 point mutants were protected from HUWE1-mediated destabilization (Fig. 6P and SI Appendix, Fig. S8J). Altogether, these data indicate that an exquisitely conserved interaction interface shared among HAPSTR1 isoforms mediates binding to HUWE1, which then promotes HAPSTR1 degradation through K48 polyubiquitination.

HUWE1 Is Required for HAPSTR1 to Control Stress Signaling.

In coessentiality analyses, such as that which served as the basis

for our stress network, E3 ligases often have markedly anticorrelated fitness profiles with substrates they mark for degradation (6, 10, 32). Examples of this in our network include MDM2 with TP53, CUL3-KEAP1 with NFE2L2, and VHL with HIF1A and EPAS1 (Fig. 1H). In stark contrast, HUWE1 and HAPSTR1 are each other's most positively correlated gene in our coessentiality analysis (Fig. 7A). We emphasize that the magnitude of the positive fitness correlation between HAPSTR1 and HUWE1 ($r = 0.49$)—among the strongest of all correlations across the genome and reproducible in an independent fitness screening dataset (Fig. 7B and SI Appendix, Fig. S8K and L)—would be highly atypical for two proteins that do not have an obligately cooperative function in the same pathway (SI Appendix, Fig. S8M) (33). For example, the only top-ranked reciprocal correlations in our network that were stronger than HAPSTR1–HUWE1 were canonical cofactors (TP53–TP53BP1 and EIF2AK4/GCN2–GCN1).

To investigate a potential cooperative role between HAPSTR1 and HUWE1, we began by knocking down each gene alone or in combination, with RNA-seq as an indirect readout of global cellular signaling. Consistent with a model of cooperation, knock-down of HAPSTR1, HUWE1, or both genes caused remarkably

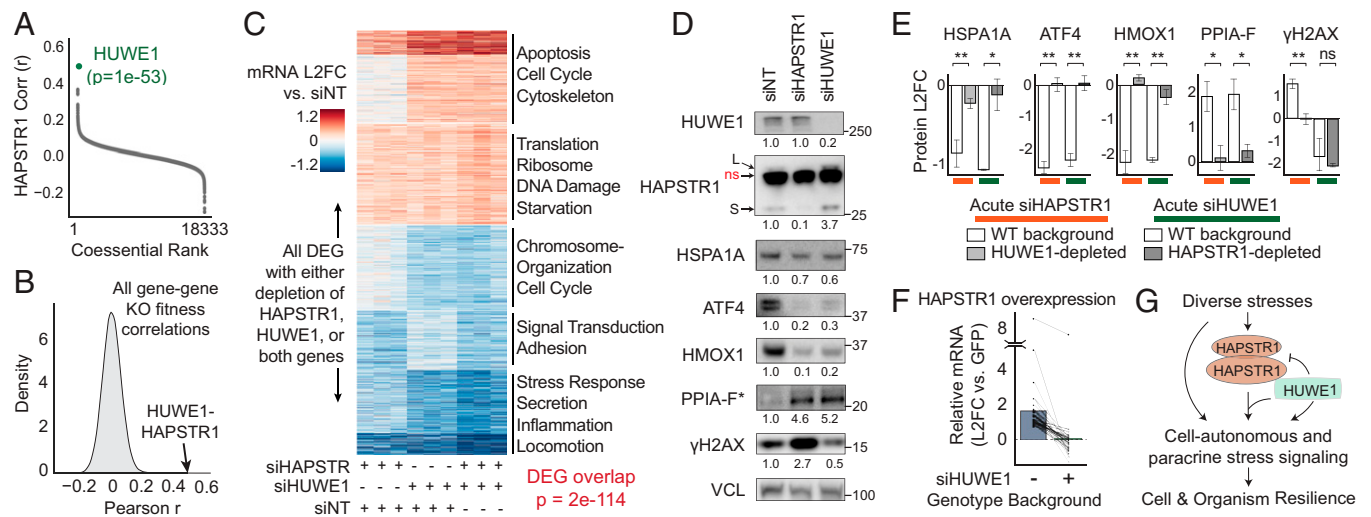


Fig. 7. HAPSTR1 cooperates with HUWE1 to control stress signaling. (A and B) HUWE1 is the most coessential gene for HAPSTR1 (A), and this relationship is markedly strong compared with all other correlations (Corr) in the genome (B). (C) Phenotypic convergence based on differentially expressed gene (DEG) overlap of HAPSTR1 and HUWE1 knockdown RNA-seq data in 231 cells. Gene set enrichment analysis terms shown (false discovery rate [FDR] < 1e-5). K-means clustering, K = 7. (D) HUWE1 depletion recapitulates the effects of HAPSTR1 loss on model signaling proteins, despite increasing HAPSTR1 levels. U2OS. L, long; S, short. *PPIA-FLAG (PPIA-F) was transfected in separate experiments. Representative blots, $n \geq 3$. (E) For five model signaling proteins, quantification of the effect of HAPSTR1 or HUWE1 depletion in cells chronically depleted of the other factor, as in *SI Appendix, Fig. S9B*, compared with acute knockdown in WT cells. * $P < 0.05$, ** $P < 0.005$, two-tailed t test. ns, not significant. (F) Genes differentially expressed (RNA-seq FDR < 0.05) in 293T cells 24 h after transient overexpression of HAPSTR1 are not regulated by HAPSTR1 overexpression in cells lacking HUWE1. (G) Schematic model of the HAPSTR1-HUWE1 pathway. GFP, green fluorescent protein; L2FC, Log₂foldchange.

similar effects on global gene expression (Fig. 7C). Particularly, genes related to protein synthesis/translation, DNA damage, and the starvation response were up-regulated by loss of either or both genes, while stress response and chemokine/secretion genes were suppressed. Similarly, at the level of proteome ubiquitination, depletion of HUWE1 or HAPSTR1 caused concordant global changes as measured by FLAG-ubiquitin IP-MS (*SI Appendix, Fig. S9A*). Finally, we confirmed that—despite increasing HAPSTR1 protein abundance—HUWE1 depletion mimicked the effects of HAPSTR1 depletion at the level of multiple cell-autonomous and paracrine stress signaling pathways (Fig. 7D). The single exception we observed is that while HAPSTR1 loss increased γ H2AX, HUWE1 loss decreased γ H2AX (Fig. 7D), the latter consistent with a recently established role for HUWE1 at stalled replication forks (34). The coessentiality and signaling data together suggest that HAPSTR1 and HUWE1 play a critical role in a shared pathway, with major consequences for global stress signaling.

Our data indicating that HUWE1 loss phenocopies HAPSTR1 loss and that codepletion of both factors provides minimal additive effect led us to further investigate the epistasis of the HUWE1-HAPSTR1 relationship. Compared with acute knockdown in WT cells, acute HAPSTR1 knockdown in cells chronically depleted of HUWE1 no longer affected model signaling proteins HSPA1A, ATF4, HMOX1, PPIA-FLAG, and γ H2AX (Fig. 7E and *SI Appendix, Fig. S9B*). Stated differently, although HAPSTR1 depletion reduces ATF4 (for example), if HUWE1 is not present, HAPSTR1 depletion causes no additional change in ATF4 protein levels. Similarly, HUWE1 was required for HAPSTR1 overexpression to affect signaling (Fig. 7F). For the most part, the effects of HUWE1 depletion on stress signaling were suppressed by chronic HAPSTR1 depletion. The one exception was γ H2AX, which was regulated differently by HUWE1 than HAPSTR1 in WT cells and was still regulated by HUWE1 in HAPSTR1-deficient cells (Fig. 7E and *SI Appendix, Fig. S9B*). Altogether, these data suggest that HUWE1 is an obligate cofactor in the pathway through which HAPSTR1 controls global stress

signaling but that HUWE1 can regulate certain proteins in a HAPSTR1-independent fashion.

Finally, we tested several biochemical mechanisms that could serve as the final step linking the HAPSTR1-HUWE1 complex with downstream signaling targets. Given the well-established role of HUWE1 as a pleiotropic E3 ligase, we examined whether HAPSTR1 acts as a cofactor for HUWE1 to recruit or ubiquitinate its substrates. In such a model, HUWE1 degradation of HAPSTR1 may serve as an autoregulatory feedback mechanism, as observed with E3 ligase autoubiquitination or targeting of complex members (35, 36). However, with or without stress, HAPSTR1 loss did not robustly stabilize canonical HUWE1 substrates such as DDIT4, MCL1, or c-MYC (*SI Appendix, Fig. S9C-E*). Additionally, we found no evidence that HAPSTR1 is essential for other processes previously associated with the HUWE1 (or yeast TOM1) E3 ligase, such as degradation of unassembled protein complex members, clearance of the ubiquitin fusion protein Ub^{G76V}-GFP, regulation of mRNA export, or facilitation of stress-induced neddylation (*SI Appendix, Fig. S9F-K*) (28, 37-40). We also found no evidence that HAPSTR1 is required for normal HUWE1 localization or for HUWE1 to interact with its typical binding partners (*SI Appendix, Fig. S9L and M*).

We therefore propose a model whereby HAPSTR1 cooperates with and is destabilized by HUWE1 in a conserved pathway that—independent from canonical HUWE1 processes—regulates an integrated network of cell-autonomous and paracrine stress signaling pathways to promote resilience (Fig. 7G).

Discussion

Organismal health requires that individual cells adapt to the complex combinations of stressors encountered during normal and abnormal physiology. This adaptability stems from a wide array of highly conserved and well-characterized stress response programs. Physiological stresses—such as those posed in cancer, aging, and neurodegeneration—invariably activate multiple

stress responses simultaneously. Thus, identification of mechanisms that centrally coordinate the cell's network of stress response systems would have implications for some of humanity's most common afflictions.

To search for central factors that oversee a global stress network, we took inspiration from yeast, where only ~20% of the genome is essential for growth in rich media, but ~97% of genes are required in at least one stress context (7). We found a similar pattern of context-specific essentiality for stress response factors in human cells, an observation that facilitated the unbiased identification of an interconnected network of factors that critically regulate different cellular stress responses. Our network nominates pathway components, suggests hierarchy among specialized effectors, and provides hints as to the triggers of pathway dependence in proliferating cells. Additionally, we identify a compendium of crosstalk genes critical for cells in multiple distinct stress states, many of which have no prior connections to stress response biology (Dataset S1). While we focused our experimental efforts on HAPSTR1, it is likely that other crosstalk genes also have important roles in the integration of multiple stress responses. Our network and source data may thus serve as a launching point for studies of these additional factors.

What, then, differentiated HAPSTR1 from other stress network genes? HAPSTR1's dynamic regulation by multiple stressors, direct network connections to multiple stress response pathways, and marked increase in essentiality among cells facing a combinatorial stress burden were suggestive of a particularly important role in global stress signaling. This inference was supported by data in human cells and nematodes, which together revealed that HAPSTR1 governs tolerance of diverse stressors and functionally tunes the output of critical stress network pathways. The potential importance of such a protein led us to biochemically dissect the uncharacterized HAPSTR1.

Our data indicate that HAPSTR1 encodes a protein with a long (1–275 aa) and short (1–198 aa) isoform. Distant orthologs of HAPSTR1, such as those found in fungi and plants, have poor sequence identity in several regions, but perfect conservation of a motif (F-x(2)-AA-x(5)-LY[KRT]-[x(12 or 16)]-G; see Fig. 3C) present in both human HAPSTR1 isoforms. This critically conserved motif, located in a region we term the HBO domain, mediates two biochemical phenotypes: oligomerization and HUWE1 binding. The functional consequences of the former phenotype remain incompletely understood. However, we emphasize that every effect we observed from depletion of both HAPSTR1 isoforms—including those as broad as transcriptome-wide signaling changes—was affected equally by depletion of just the full-length isoform. One possible explanation for this finding, supported by the perfect conservation of G119 (which enables oligomerization and promotes protein stability) is that HAPSTR1 requires oligomerization between isoforms for proper function.

The second phenotype enabled by the key residues in the HBO domain is HAPSTR1's intriguing and multifaceted physical interaction with HUWE1. HUWE1 is the most enriched binding partner for HAPSTR1 by IP-MS, with several orthogonal experiments demonstrating a strong and consistent interaction that does not require exogenous stress. One functional consequence of this interaction is that HUWE1 can assemble K48-linked ubiquitin chains on HAPSTR1 to promote its degradation. We note that, unlike several other HUWE1 substrates that are regulated by HUWE1 only in specific conditions (31), HUWE1 appears to regulate HAPSTR1 robustly regardless of the cell line or stress environment. Thus, HAPSTR1 dysregulation is likely present in each of the myriad clinical disorders associated with alterations in HUWE1.

Although our data indicate that HUWE1 directly promotes HAPSTR1 degradation, multiple lines of evidence suggest that the relationship between HUWE1 and HAPSTR1 is not simply antagonistic. Phenotypically, CRISPR-Cas9 deletion of either HAPSTR1 or HUWE1 results in a highly similar dependency profile across hundreds of cell lines, a pattern starkly unusual for any two proteins that do not cooperate in the same biochemical pathway. Evolutionarily, the key residues in HAPSTR1's exquisitely conserved motif are each required for efficient HUWE1 binding. At the molecular level, HAPSTR1 and HUWE1 control stress signaling nearly identically across diverse cell lines. Finally, considering epistasis, codepletion of both HAPSTR1 and HUWE1 mimics depletion of the individual factors, and HUWE1 must be present for HAPSTR1 depletion or overexpression to alter signaling. Thus, while HUWE1 directly mediates HAPSTR1 degradation, our data indicate that HUWE1 is also a required cofactor in the pathway by which HAPSTR1 governs stress signaling.

While we have been unable to identify HAPSTR1 phenotypes that do not require HUWE1, we did observe certain HUWE1 phenotypes that did not require HAPSTR1 (i.e., regulation of DDIT4 and γ H2AX). That HUWE1 has certain HAPSTR1-independent functions may explain why, unlike HAPSTR1, HUWE1 is essential even in unstressed cells, as well as why HUWE1 controls certain genotoxic responses differently from HAPSTR1 (SI Appendix, Fig. S10A–C). This distinction may have clinical relevance. That is, HUWE1 has garnered substantial attention as a potential therapeutic target in fields from oncology to neurology and cardiology. However, the extreme breadth of HUWE1 substrates—deregulation of which as an ensemble can cause severe and unpredictable effects on cellular function—pose major challenges for efficacy and tolerability. Specifically, HUWE1 modulation causes context-dependent (and sometimes conflicting) effects in ostensibly similar disease models (41), and the nature of HUWE1 as a pan-essential gene suggests that HUWE1-targeted therapies are unlikely to escape systemic toxicity (42). Thus, our observation that HAPSTR1 mediates a major function of HUWE1 suggests that HAPSTR1 may represent a mechanism to access a disease-relevant function of HUWE1 with a more favorable therapeutic window.

The critical remaining question is how specifically the HAPSTR1–HUWE1 complex mediates control over their shared array of signaling targets. The most parsimonious explanation employs HUWE1's activity as a ubiquitin ligase, with HAPSTR1 acting as a HUWE1 cofactor that is degraded through autoregulatory feedback (35, 36). However, we have yet to identify any substrates that are robustly and consistently modified by HUWE1 in a HAPSTR1-dependent fashion. Thus, while as yet unidentified proteins that are ubiquitinated by the HAPSTR1–HUWE1 complex may exist, it is also possible that HAPSTR1 is the primary effector of the HAPSTR1–HUWE1 pathway; that is, HAPSTR1 may have an independent activity that must be tightly controlled, with transcriptional stress-induction and HUWE1-mediated degradation acting as titration mechanisms. It is also tempting to speculate that the targeting of HAPSTR1 to the proteasome by HUWE1 serves a functional purpose and is not simply a mechanism of feedback antagonism.

Altogether, our data provide insight into a fundamental question—how the diverse array of response pathways employed by stressed cells are coordinately and centrally regulated. We propose that HAPSTR1 is a rheostat centrally poised to oversee an integrated network of coregulated pathways, modulation of which may have broad implications for human health and disease.

Materials and Methods

Modified coessentiality analyses were performed as previously described (10). Biochemical experiments followed standard protocols. See [SI Appendix](#) for greater detail.

Data Availability. All study data are included in the supporting information and/or have been uploaded to Gene Expression Omnibus ([GSE204961](#)) (43).

ACKNOWLEDGMENTS. We thank Dr. Eva Gottwein, Dr. Navdeep Chandel, Michael R. Drumm, Bettina H. Cheung, and Sage L. Morison for comments on the manuscript. We thank Dr. Clara B. Peek and Dr. Yoko Shibata for helpful discussions and Dr. Elizabeth Bartom for developing the Ceto bioinformatics pipeline (<https://github.com/ebartom/NGSbartom>). We thank Dr. Manabu Kurokawa (Kent State University) for graciously providing the HUWE1-C4341S construct. D.R.A. was supported by the NIH (Grant Nos. F30CA264513, T32GM008152). M.L.M. was supported by the NIH (Grant No. R00CA175293) and the American Cancer Society (Grant Nos. IRG-18-163-24 ABOA Impact, RSG-22-086-01-TBE).

1. S. Fulda, A. M. Gorman, O. Hori, A. Samali, Cellular stress responses: Cell survival and cell death. *Int. J. Cell Biol.* **2010**, 214074 (2010).
2. M. Costa-Mattoli, P. Walter, The integrated stress response: From mechanism to disease. *Science* **368**, eaat5314 (2020).
3. L. Galluzzi, T. Yamazaki, G. Kroemer, Linking cellular stress responses to systemic homeostasis. *Nat. Rev. Mol. Cell Biol.* **19**, 731–745 (2018).
4. J. Luo, N. L. Solimini, S. J. Elledge, Principles of cancer therapy: Oncogene and non-oncogene addiction. *Cell* **136**, 823–837 (2009).
5. A. Tsherniak *et al.*, Defining a cancer dependency map. *Cell* **170**, 564–576.e16 (2017).
6. T. Wang *et al.*, Gene essentiality profiling reveals gene networks and synthetic lethal interactions with oncogenic Ras. *Cell* **168**, 890–903.e15 (2017).
7. M. E. Hillenmeyer *et al.*, The chemical genomic portrait of yeast: Uncovering a phenotype for all genes. *Science* **320**, 362–365 (2008).
8. R. M. Meyers *et al.*, Computational correction of copy number effect improves specificity of CRISPR-Cas9 essentiality screens in cancer cells. *Nat. Genet.* **49**, 1779–1784 (2017).
9. M. Calfon *et al.*, IRE1 couples endoplasmic reticulum load to secretory capacity by processing the XBP-1 mRNA. *Nature* **415**, 92–96 (2002).
10. D. R. Amici *et al.*, FIREWORKS: A bottom-up approach to integrative coessentiality network analysis. *Life Sci. Alliance* **4**, e202000882 (2020).
11. M. Dede, M. McLaughlin, E. Kim, T. Hart, Multiplex enCas12a screens detect functional buffering among paralogs otherwise masked in monogenic Cas9 knockout screens. *Genome Biol.* **21**, 262 (2020).
12. C. J. Huggins *et al.*, C/EBP γ is a critical regulator of cellular stress response networks through heterodimerization with ATF4. *Mol. Cell. Biol.* **36**, 693–713 (2015).
13. H. Motohashi, F. Katsuoka, J. D. Engel, M. Yamamoto, Small Maf proteins serve as transcriptional cofactors for keratinocyte differentiation in the Keap1-Nrf2 regulatory pathway. *Proc. Natl. Acad. Sci. U.S.A.* **101**, 6379–6384 (2004).
14. J. Huang, B. D. Manning, The TSC1-TSC2 complex: A molecular switchboard controlling cell growth. *Biochem. J.* **412**, 179–190 (2008).
15. M. Hutchison, K. S. Berman, M. H. Cobb, Isolation of TAO1, a protein kinase that activates MEKs in stress-activated protein kinase cascades. *J. Biol. Chem.* **273**, 28625–28632 (1998).
16. G. L. Johnson, K. Nakamura, The c-jun kinase/stress-activated pathway: Regulation, function and role in human disease. *Biochim. Biophys. Acta* **1773**, 1341–1348 (2007).
17. Y. Daniely, D. D. Dimitrova, J. A. Borowiec, Stress-dependent nucleolin mobilization mediated by p53-nucleolin complex formation. *Mol. Cell. Biol.* **22**, 6014–6022 (2002).
18. J. Mistry *et al.*, Pfam: The Protein Families Database in 2021. *Nucleic Acids Res.* **49** (D1), D412–D419 (2021).
19. F. M. Behan *et al.*, Prioritization of cancer therapeutic targets using CRISPR-Cas9 screens. *Nature* **568**, 511–516 (2019).
20. N. Hustedt *et al.*, A consensus set of genetic vulnerabilities to ATR inhibition. *Open Biol.* **9**, 190156 (2019).
21. M. Olivieri *et al.*, A genetic map of the response to DNA damage in human cells. *Cell* **182**, 481–496.e21 (2020).
22. Y. Lai *et al.*, Illuminating host-mycobacterial interactions with genome-wide CRISPR knockout and CRISPRi screens. *Cell Syst.* **11**, 239–251.e7 (2020).

M.L.M. was also supported by Kimmel Scholar (Grant No. SKF-16-135) and Lynn Sage Scholar awards. The Northwestern Proteomics Core Facility was supported by the NIH (Grant Nos. P30CA060553, S100D025194, P41GM108569). D.R.F. was supported by the NIH (Grant No. R01GM111907). J.L. was supported by the NIH (Grant Nos. R35GM138364, 5P20GM103636). This project was supported by a Robert H. Lurie Comprehensive Cancer Center H Foundation Collaboration Award.

Author affiliations: ^aSimpson Querrey Center for Epigenetics and Department of Biochemistry and Molecular Genetics, Northwestern University Feinberg School of Medicine, Chicago, IL 60610; ^bRobert H. Lurie Comprehensive Cancer Center, Northwestern University Feinberg School of Medicine, Chicago, IL 60610; ^cFunctional and Chemical Genomics Research Program, Oklahoma Medical Research Foundation, Oklahoma City, OK 73104; and ^dNorthwestern Proteomics Center of Excellence Core Facility, Northwestern University, Evanston, IL 60208

Author contributions: D.R.A., J.L., and M.L.M. designed research; D.R.A., D.J.A., K.A.M., R.S.S., C.M.P., S.G., S.S., T.C., S.L.E., S.B., S.R.T., B.P.O., B.-K.C., and J.L. performed research; D.R.A., D.J.A., K.A.M., C.M.P., S.G., T.C., S.L.E., N.L.K., I.B.-S., D.R.F., J.L., and M.L.M. contributed new reagents/analytic tools; D.R.A., T.C., S.L.E., B.-K.C., Y.A.G., and J.L. analyzed data; and D.R.A. and M.L.M. wrote the paper.

23. Y. Benslimane *et al.*, Genome-wide screens reveal that resveratrol induces replicative stress in human cells. *Mol. Cell* **79**, 846–856.e8 (2020).
24. J. Han *et al.*, Genome-wide CRISPR/Cas9 screen identifies host factors essential for influenza virus replication. *Cell Rep.* **23**, 596–607 (2018).
25. Y. Benslimane *et al.*, A novel p53 regulator, C16orf72/TAPR1, buffers against telomerase inhibition. *Aging Cell* **20**, e13331 (2021).
26. J. Suzuki, Z. G. Jin, D. F. Meoli, T. Matoba, B. C. Berk, Cyclophilin A is secreted by a vesicular pathway in vascular smooth muscle cells. *Circ. Res.* **98**, 811–817 (2006).
27. M. K. Sung *et al.*, A conserved quality-control pathway that mediates degradation of unassembled ribosomal proteins. *eLife* **5**, e19105 (2016).
28. J. Jumper *et al.*, Highly accurate protein structure prediction with AlphaFold. *Nature* **596**, 583–589 (2021).
29. M. Mirdita *et al.*, ColabFold: Making protein folding accessible to all. *Nat. Methods* **19**, 679–682 (2022).
30. M. Hunkeler *et al.*, Solenoid architecture of HUWE1 contributes to ligase activity and substrate recognition. *Mol. Cell* **81**, 3468–3480.e7 (2021).
31. S. H. Kao, H. T. Wu, K. J. Wu, Ubiquitination by HUWE1 in tumorigenesis and beyond. *J. Biomed. Sci.* **25**, 67 (2018).
32. E. Kim *et al.*, A network of human functional gene interactions from knockout fitness screens in cancer cells. *Life Sci. Alliance* **2**, e201800278 (2019).
33. J. Pan *et al.*, Interrogation of mammalian protein complex structure, function, and membership using genome-scale fitness screens. *Cell Syst.* **6**, 555–568.e7 (2018).
34. K. N. Choe *et al.*, HUWE1 interacts with PCNA to alleviate replication stress. *EMBO Rep.* **17**, 874–886 (2016).
35. M. E. R. Maitland *et al.*, The mammalian CTLH complex is an E3 ubiquitin ligase that targets its substrate muskellin for degradation. *Sci. Rep.* **9**, 9864 (2019).
36. P. de Bie, A. Ciechanover, Ubiquitination of E3 ligases: Self-regulation of the ubiquitin system via proteolytic and non-proteolytic mechanisms. *Cell Death Differ.* **18**, 1393–1402 (2011).
37. E. G. Poulsen *et al.*, HUWE1 and TRIP12 collaborate in degradation of ubiquitin-fusion proteins and misfolded ubiquitin. *PLoS One* **7**, e50548 (2012).
38. C. M. Maghames *et al.*, NEDDylation promotes nuclear protein aggregation and protects the ubiquitin proteasome system upon proteotoxic stress. *Nat. Commun.* **9**, 4376 (2018).
39. N. Iglesias *et al.*, Ubiquitin-mediated mRNA dynamics and surveillance prior to budding yeast mRNA export. *Genes Dev.* **24**, 1927–1938 (2010).
40. Y. Xu, D. E. Anderson, Y. Ye, The HECT domain ubiquitin ligase HUWE1 targets unassembled soluble proteins for degradation. *Cell Discov.* **2**, 16040 (2016).
41. X. Gong *et al.*, The structure and regulation of the E3 ubiquitin ligase HUWE1 and its biological functions in cancer. *Invest. New Drugs* **38**, 515–524 (2020).
42. L. Chang, P. Ruiz, T. Ito, W. R. Sellers, Targeting pan-essential genes in cancer: Challenges and opportunities. *Cancer Cell* **39**, 466–479 (2021).
43. D. R. Amici, L. Mendillo, Sequencing data accompanying “C16orf72/HAPSTR1 is a molecular rheostat in an integrated network of stress response pathways.” Gene Expression Omnibus. <https://www.ncbi.nlm.nih.gov/geo/query/acc.cgi?acc=GSE204961>. Deposited 26 May 2022.